Published in final edited form as:
Biochim Biophys Acta. 2008 October ; 1783(10): 1866–1875. doi:10.1016/j.bbamcr.2008.05.010.

CAVEOLAE ARE AN ESSENTIAL COMPONENT OF THE PATHWAY FOR ENDOTHELIAL CELL SIGNALING ASSOCIATED WITH ABRUPT REDUCTION OF SHEAR STRESS

Tatyana Milovanova,
Institute For Environmental Medicine, University of Pennsylvania Medical Center, One John Morgan Building, Philadelphia, PA 19104-6068.

Shampa Chatterjee,
Institute For Environmental Medicine, University of Pennsylvania Medical Center, One John Morgan Building, Philadelphia, PA 19104-6068.

Brian J. Hawkins,
Institute For Environmental Medicine, University of Pennsylvania Medical Center, One John Morgan Building, Philadelphia, PA 19104-6068.

NanKang Hong,
Institute For Environmental Medicine, University of Pennsylvania Medical Center, One John Morgan Building, Philadelphia, PA 19104-6068.

Elena M. Sorokina,
Institute For Environmental Medicine, University of Pennsylvania Medical Center, One John Morgan Building, Philadelphia, PA 19104-6068.

Kris DeBolt,
Institute For Environmental Medicine, University of Pennsylvania Medical Center, One John Morgan Building, Philadelphia, PA 19104-6068.

Jonni S. Moore,
Abramson Cancer Center Flow Cytometry and Cell Sorting Shared Resources, University of Pennsylvania Medical Center, One John Morgan Building, Philadelphia, PA 19104-6068.

Muniswamy Madesh, and
Institute For Environmental Medicine, University of Pennsylvania Medical Center, One John Morgan Building, Philadelphia, PA 19104-6068.

Aron B. Fisher
Institute For Environmental Medicine, University of Pennsylvania Medical Center, One John Morgan Building, Philadelphia, PA 19104-6068.

Abstract

Address for Correspondence: Aron B. Fisher, M.D., Institute for Environmental Medicine, University of Pennsylvania Medical Center, One John Morgan Building, Philadelphia, PA 19104-6068. Phone: 215-898-9100; FAX: 215-898-0868, E-mail: abf@mail.med.upenn.edu.

Abrupt cessation of flow representing the acute loss of shear stress (simulated ischemia) to flow-adapted pulmonary microvascular endothelial cells (PMVEC) leads to reactive oxygen species (ROS) generation that signals for EC proliferation. We evaluated the role of caveolin-1 on this cellular response with mouse PMVEC that were preconditioned for 72 h to laminar flow at 5 dynes/cm^2 followed by stop of flow ("ischemia"). Preconditioning resulted in a 2.7-fold increase in cellular expression of K_{ATP} (K_{IR} 6.2) channels but no change in expression level of caveolin-1, gp91^{phox}, or MAP kinases. The initial response to ischemia in wild type cells was cell membrane depolarization that was abolished by gene targeting of K_{IR} 6.2. The subsequent response was increased ROS production associated with activation of NADPH oxidase (NOX2) and then phosphorylation of MAP kinases (Erk, JNK). After 24 h of ischemia in wild type cells, the cell proliferation index increased 2.5 fold and the % of cells in S+G_2/M phases increased 6-fold. This signaling cascade (cell membrane depolarization, ROS production, MAP kinase activation and cell proliferation) was abrogated in caveolin-1 null PMVEC or by treatment of wild type cells with filipin. These studies indicate that caveolin-1 functions as a shear sensor in flow-adapted EC resulting in ROS-mediated cell signaling and endothelial cell proliferation following the abrupt reduction in flow.

Keywords

shear stress; mechanotransduction; K_{ATP} channel; NADPH oxidase; pulmonary microvascular endothelium; reactive oxygen species; cell proliferation

INTRODUCTION

We have shown, initially with studies of the isolated perfused lung and subsequently with endothelial cells *in vitro*, that acute cessation of pulmonary perfusion results in increased production of reactive oxygen species (ROS) by pulmonary endothelial cells as part of a signaling cascade associated with altered mechanical stress [1–8]. The loss of this response with deletion of gp91^{phox} indicated that the source of ROS is the endothelial cell NADPH oxidase and specifically the isoform that is now called NOX2 [4,6,8]. One consequence of this signaling cascade that was demonstrated with the *in vitro* model of ischemia is ROS-mediated endothelial cell proliferation [5–7]. We have postulated that this physiological event represents nascent angiogenesis to compensate for the loss of blood flow. Recent studies have suggested that caveolae in the cell membrane may respond to altered mechanotransduction [9–11] and led us to postulate that these organelles could be a primary sensor for ischemia and for initiation of subsequent cellular signaling events.

The goals of the present study were to investigate the role of caveolin-1 protein and caveolae in activation of ROS production and microvascular cell proliferation associated with loss of shear stress (ischemia). We evaluated microvascular endothelium *in situ* using both the isolated perfused lung and an *in vitro* model of the pulmonary microvascular endothelium. For the latter, pulmonary microvascular endothelial cells in culture were pre-adapted to shear stress thereby simulating their *in situ* physiological state. These studies have relevance for understanding the endothelial cell response to acute ischemia and the basis for altered mechanotransduction such as might be associated with a pulmonary embolism, lung transplantation, or other pathologies that result in abrupt cessation of pulmonary perfusion.

MATERIALS AND METHODS

Materials and animals

Fluorescent probes were 2',7'-dichlorofluorescein (H_2DCF) diacetate (Kodak, Rochester, NY), bisoxonol, Dil-acetylated low density lipoprotein (DilAcLDL), Alexa Fluor 488 AcLDL and amplex red/horseradish peroxidase (Molecular Probes, Eugene, OR). Inhibitors and

agonists used were thrombin, Na_3VO_4, okadaic acid and filipin (Sigma, St. Louis, MO), cyclosporine A (Alexis, San Diego, CA), and nocodazole, 2-(2-amino-3-methoxyphenyl) -4H-1-benzopryan-4-one (PD98059) and 1,4-diamino-2,3-dicyano-1,4-bis[2-aminophenylthio] butadiene (UO126) (Calbiochem, San Diego, CA). Antibodies used were anti-CD31 conjugated with fluorescein isothiocyanate (FITC) (Caltag, Burlingame, CA); anti-Kir 6.2 polyclonal (Alomone, Jerusalem, Israel); anti-gp91^{phox} monoclonal, anti-caveolin-1 FITC polyclonal, anti-p38MAPK, anti-p-P38MAPK and anti-VE cadherin (BD Biosciences, Pharmingen); anti-ERK1/2, anti-p-ERK1/2, anti-JNK1/2, anti-p-JNK1/2 and anti-caveolin-1 monoclonal (Santa Cruz Biotechnology, Santa Cruz, CA); and anti-Factor VIII (Accurate Chem, Westbury, NY)

C57Bl/6 (wild-type), caveolin-1−/− (stock #4585), and gp91phox −/− (stock #2365) mice were obtained from the Jackson Laboratory (Bar Harbor, ME); Kir6.2−/− mice were bred in our facility from breeding pairs supplied by Dr. S. Seino (Chiba University, Chiba, Japan). The gp91^{phox} and K_{IR} 6.2 null mice are on the C57Bl/6 background. The caveolin-1 null mice are on a mixed background (C57 Bl/6, 129/Sv and SJL). These latter mice have been shown to lack plasmalemmal caveolae in endothelial cells [12]. All procedures involving the use of mice were approved by the Institutional Animal Care and Use Committee.

Imaging of the isolated perfused lung

Imaging of the isolated perfused lung was carried out with minor modifications of the procedure as described previously [3]. Mice were anesthetized with 50 mg/kg intraperitoneal sodium pentobarbital and continuously ventilated through a tracheal cannula with 5% CO_2 in air (BOC group Inc. Murray Hill, NJ, USA). The chest was opened and the pulmonary circulation was cleared of blood by gravity flow of perfusion through a cannula inserted in the main pulmonary artery, exiting from the transected left ventricle. The perfusate was Krebs Ringer bicarbonate solution (KRB: NaCl 118.45, KCl 4.74, $MgSO_4$.7H2O 1.17, KH_2PO_4 1.18 and $NaHCO_3$ 24.87 mM) supplemented with 10mM glucose and 5% dextran to maintain osmolarity. The lung preparation was placed onto a chamber on the stage of a two photon scanning microscope (BioRad radiance 2000 confocal microscope, Hercules, CA, with a coherent minor 900 high sapphire laser pump) for in situ imaging. The microscope was equipped with an optical filter changer (lambda 10–2; Sutter Instrument Co. Novato, CA), a Nikon Eclipse TE-300 digital camera (Melville, NY) and LaserSharp 2000 image acquisition software (BioRad, Hercules, CA). The Ti-sapphire source of the two-photon system is a laser that produces photon pulses at femtosecond intervals. The laser beam allows for penetration up to 150–200 μm below the lung surface at the wavelengths used for measurement of amplex red and Alexa AcLDL.

For outlining the endothelium, the isolated perfused lung was pre-perfused with AlexaAcLDL (1 μg/ml) for 30 min to allow for the uptake of the fluorophore, and the intravascular dye was removed by 10 min perfusion with dye free buffer. For imaging ROS, lungs were preperfused with amplex red (25 μM) plus horseradish peroxidase (25 μg/ml) in order to detect H_2O_2 in the intravascular space. Perfusion into the pulmonary artery in the preparation was maintained by a peristaltic pump generally at a flow rate of 2 ml/min. Ischemia was simulated by stop of perfusate flow and endothelium was imaged for the subsequent 5 min. Ventilation was maintained throughout the experiment and stopped only at the point of image capture. For each experiment, scanning was focused on those vessels which could be best visualized due to their optimal location. For each mouse, 3–4 fields were selected randomly for fluorescence quantification.

Cell isolation and Cell Culture

Pulmonary microvascular endothelial cells (MPMVEC) were isolated from lungs as described previously [6,13,14]. Briefly, freshly harvested mouse lungs were treated with collagenase

followed by isolation of cells by adherence to magnetic beads (Dynabeads, Dynal, Oslo, Norway) coated with mAb (anti-CD31) to platelet endothelial cell adhesion molecule (PECAM). MPMVEC were propagated in Dulbecco's modified Eagle medium (DMEM) supplemented with 10% fetal bovine serum (FBS), non-essential amino acids, and penicillin/streptomycin and maintained under static culture conditions. The endothelial phenotype of the preparation was routinely confirmed by evaluating cellular uptake of DiIAcLDL and by immunostaining for PECAM (CD31), VE-cadherin, von Willebrand factor (factor VIII), caveolin-1, and vascular endothelial growth factor (VEGF) receptor-1 (flt1) and -2 (flk1). Cells were evaluated by both fluorescence microscopy and flow cytometry using the FACSCalibur as described below. A549 cells from American Type Culture Collection (Manassas, VA) were used as a negative control for immunostaining.

Flow adaptation and simulated ischemia

Cells were flow adapted during culture in an artificial capillary system using previously described methods [5–7,14]. MPMVEC between passages 5–14 were seeded at a confluent density (14–18 × 10^6 cells per cartridge) and allowed 24 h for attachment. Cells then were cultured under flow of culture medium (Dulbeccos's modified Eagle medium, DMEM) using commercially available artificial capillary technology (FiberCell Systems, Frederick, MD). Flow adaptation in cartridges generally was carried out for 72 h at 5 dynes/cm^2 shear stress. The nominal times indicated in this report do not include the initial 24 h attachment period used for all experiments. For fluorescence imaging studies, the fluorophore was added to the perfusate during the final 1 h of the flow-adaptation period. Cells then were subjected to either 1 h of additional continuous flow (control) or 1 h of simulated ischemia. The perfusate during the loading and experimental periods was changed from DMEM to Krebs-Ringer bicarbonate (KRB) solution, pH7.4, supplemented with 10 mM glucose, 25 mM HEPES, and 3% dextran. "Ischemia" was simulated by rerouting the flow from the luminal to the abluminal compartment. This protocol eliminated shear stress but allowed continued oxygenation and substrate delivery. For studies of cell proliferation, cells were grown under either flow or static conditions for 96 h while cells for study of ischemia were grown under flow for 72 h followed by 24 h of no flow. Cells were removed from the cartridges by treatment with 0.25% trypsin or Accutase® (Chemicon International, Temecula, CA) for 5–10 min, and pelleted by centrifugation at 1,400g at 4°C for 5 min. Cells were analyzed by flow cytometry, Western blot, and confocal microscopy.

Membrane depolarization with ischemia

Membrane depolarization was detected by live cell imaging using a cell membrane potential probe [15,16]. MPMVEC in Dulbecco's modified Eagle medium were plated on a glass slide (44 × 20 mm) that had been coated with 0.2% gelatin. When cells were fully confluent, the slide was placed in a laminar flow chamber (Confocal Imaging chamber RC-30, Warner Instruments, Hamden, CT) and maintained under static or continuous laminar flow (5 dyn/cm^2) at 37°C for 24 h. For experimental measurements, the growth medium was substituted with supplemented Krebs-Ringer bicarbonate buffer. Cells in the flow chamber were perfused with the membrane potential-sensitive fluorophore bis-oxonol (200 nM) for 30 min and imaged before and after flow cessation. Excitation for fluorescence imaging was accomplished with a mercury lamp fiber-optic light source and appropriate filter set: HQ-41001 with 480 ± 20 nm excitation, 505LP dichroic, and 535 ± 25 nm emission (Chroma Technology, Brattleboro, VT). For quantitation, areas of interest were randomly selected, and fluorescence intensity of each was measured and normalized as a percent change in intensity level from baseline. Endothelial depolarization by incubation with medium containing 24 mM KCl was used to provide a positive control; the Na^+ concentration in high K^+ solutions was adjusted to maintain isomolarlity.

ROS generation with ischemia

ROS generation was assessed by both fluorescence imaging and flow cytometry as described previously [5–7,14]. Cells were pre-loaded in the flow cartridges with 10 μM H_2DCF and its conversion to fluorescent dichlorofluorescein (DCF) was measured. H_2DCF was used as the diacetate to promote cell entry. This compound is de-esterified intracellularly to generate the free probe. DCF fluorescence of the harvested cells was evaluated by confocal microscopy (Radiance 2000, BioRad, Hercules, CA) at 530 nm (excitation at 490 nm). The number of cells in the microscopic field was determined using ImagePro software (Media Cybernetics, Silver Spring, MD). DCF fluorescence also was evaluated by flow cytometry using a 4-color, dual laser FACSCalibur (Becton Dickinson, San Jose, CA). Excitation was by a 488 nm argon laser and light was collected using a 530±15nm bandpass filter [5].

Cell Proliferation and Cell Cycle Analysis

Cell proliferation was studied by labeling endothelial cells with PKH26, a lipid soluble dye that localizes in cell membranes, and analyzed by flow cytometry as described previously [5, 17]. Cells showed >95% labeling efficiency. All events were plotted in a CD31-FITC vs. side scatter plot (SSC-H) and a gate was set around the CD31 positive cells to capture the endothelial cell population [5]. Compensation for PKH26 was concentration dependent and was determined empirically. Quantitative analysis of cell proliferation was performed by collecting 5×10^4 events and calculated using CellQuest™ acquisition/analysis software (Becton Dickinson) and the Proliferation Wizard™ module of the ModFit LT™ Macintosh program (Verity Software House, Topsham, Maine).

For cell cycle analysis, MPVEC (1×10^6) were pelleted and incubated with RNAase (100 μg/ml) and propidium iodide (4μg/ml) in Tris buffer (pH7.6) with Nonidet P40 (0.2%) at 4°C. Cell cycle phases were analyzed by flow cytometry and the percent of cells in each phase of the cell cycle was calculated based on cellular DNA content using the ModFit program. The tetraploid and aneuploid populations, as defined by their abnormal content of DNA, were excluded from the calculations.

Western blot analysis

Western blotting utilized the two-color Odyssey™ LI-COR (Lincoln, NE) technique as previously described [17]. Quantitiation of bands is based on measurement of fluorescence. Secondary dual-labeled antibodies were IrDye 800™ goat anti-rabbit (Rockland, Gilberstville, PA for the green 800nm channel) and Cy5.5 or Alexa 680 goat anti-mouse (Molecular Probes, Eugene, OR, for the red 700nm channel). For protein assay, cell pellets were resuspended in a solution of 50 mM potassium phosphate, 0.1 mM EDTA, and 0.1% 3-[(3-chloramidopropyl) dimethylammonio]-1-propansulfonate buffer (pH 7.0). The cells were sonicated on ice using a probe sonicator by two bursts of 15 s each with a 110s interval at 40% of maximum output. Cell sonicate protein concentration was determined by Coomassie blue assay (BioRad, Richmond, CA) with bovine IgG as the standard.

Statistics

Results are expressed as the mean±SE for three or more independent experiments. Significance was determined by ANOVA or *t* test as appropriate using SigmaStat (Jandel Scientific, San Jose, CA), and the level of statistical significance was defined as $P < 0.05$.

RESULTS

ROS production by endothelium in situ

Consistent with our previous studies [3], imaging of the isolated lung from wild type mice showed increase of amplex red fluorescence with ischemia indicating the generation of ROS (Fig. 1A). The red dye marker for ROS showed co-localization with Alexa acetylated LDL, a green marker for endothelium, as indicated by the yellow color in the overlay panel (Fig. 1A). The increase in endothelial fluorescence with ischemia was time-dependent and reached an apparent plateau at ~4–5 mins (Fig 1B). Increased endothelial fluorescence with ischemia was not observed in the caveolin -1 null mouse lungs (Fig 1A, B). Further studies to demonstrate the mechanism for the loss of response to ischemia were carried out using our ischemia models with isolated cells.

Phenotype of MPMVEC

The endothelial phenotype of isolated endothelial cells was evaluated by immunohistochemical analysis and flow cytometry expression of CD31, VE-cadherin, factor VIII, flt-1, flk-1 and uptake of Dil-Ac-LDL by immunofluorescence. Both wild type and caveolin 1 −/− cells were positive for all 5 antigens and demonstrated uptake of DiI-Ac-LDL, confirming the endothelial phenotype (Fig. 2A, B). The endothelial phenotype for our preparations of $gp91^{phox}$−/− and K^{IR} 6.2−/− pulmonary microvascular endothelial cells has been demonstrated previously [17] and results were confirmed in the present study (not shown). Caveolin-1 expression was detected in wild type endothelial cells by immunohistochemistry (Fig. 2A) and western blot (22kDa, Fig. 2C) but was absent in caveolin-1−/− cells. Western blot confirmed the presence of caveolin-1 and absence of $gp91^{phox}$ (58 kDa) in the $gp91^{phox}$ null cells and of K_{IR} 6.2 (37 kDa) in the K_{IR} 6.2 null cells (Fig. 2C).

Parameters for flow adaptation

In order to determine the optimal parameters for flow adaptation, cells in the cartridges were subjected to 5 dyn/cm^2 shear stress for 24–72 h or varying shear stress (1–10 dyn/cm^2) for 72 h. Measurement of ROS production (by DCF fluorescence) or cell proliferation (by PKH26) using FACS analysis for both showed essentially maximal response at 5 dyn/cm^2 for 72 h (Fig. 3) and this regimen was used for subsequent studies. This response for ROS production for mouse pulmonary microvascular cells indicated a slightly longer duration of flow exposure and higher shear stress for maximal effect as compared to our previous studies with bovine pulmonary artery endothelial cells [7]. Western blot analysis of flow adapted vs. cells cultured under static conditions showed a 3.1-fold increase in K_{IR} 6.2 expression (Table 1) as we have demonstrated previously using rat pulmonary microvascular endothelial cells [18]. The K_{IR} 6.2 expression level increased only 1.4-fold (not statistically significant) in caveolin-1 null cells with this flow adaptation protocol (not shown). The expression levels of caveolin-1, $gp91^{phox}$, Erk 1/2 and JNK 1/2 did not change with flow adaptation of wild type cells (Table 1) or caveolin-1 null cells (not shown).

Endothelial cell membrane potential during ischemia

Based on our previous observations [3,13,15,19,20], we investigated the change in cell membrane potential of MPMVEC with ischemia using bis-oxonol as the reporter fluorophore. Consistent with our previous results, flow-adapted wild type MPMVEC showed an increase in bis-oxonol fluorescence after flow cessation compatible with membrane depolarization (Fig. 4). The change in bis-oxonol fluorescence with ischemia was attenuated in K_{IR} 6.2 null cells as shown previously [15,19] and was essentially absent in caveolin-1 null MPMVEC (Fig. 4). To evaluate whether these populations of null cells could manifest a change in membrane potential with an appropriate stimulus, MPMVEC cultured under static conditions were

incubated with a solution containing a high concentration of KCl (24mM). An increase in bis-oxonol fluorescence was observed for both wild type and caveolin-1 null MPMVEC but the response in K_{IR} 6.2 null MPMVEC was greatly attenuated (Fig. 4). In contrast to the response to ischemia, the increase in bis-oxonol fluorescence in the presence of KCl was similar for wild type and caveolin -1 MPMVEC (Fig. 4). These results indicate that caveolae are required for the cell membrane depolarization response to ischemia.

ROS production with ischemia by MPMVEC in vitro

Oxidation of H_2DCF to fluorescent DCF was used to evaluate cellular generation of ROS in the isolated cell model. H_2DCF was used instead of amplex red as the latter is an extracellar fluorophore. DCF fluorescence by confocal microscopy was at a relatively low level in MPMVEC studied during flow (with a brief, ~ 5 min, ischemic period required for removal of cells from the cartridges), but increased markedly during 1 h ischemia as detected by confocal microscopy and flow cytometry (Fig. 5A, B and C). By contrast, there was no DCF oxidation with ischemia in caveolin-1−/− MPMVEC (Fig. 5A, B, C) consistent with the results obtained with the intact isolated lung (Fig. 1). ROS production with ischemia also was not seen in MPMVEC that were pretreated with flilipin (Fig. 5A, B, C), a membrane-impermeable cholesterol-binding drug that results in disruption of caveoli.

We evaluated the effect of thrombin on DCF oxidation to confirm that caveolin -1 −/− cells do possess an intact NADPH oxidase and that loss of oxidase expression did not account for the failure to produce ROS with ischemia. Wild type MPMVEC showed ROS generation when stimulated with thrombin (Fig. 5D), an agent known to activate NADPH oxidase [21] while $gp91^{phox}$ –/– cells did not respond, compatible with absence of the flavoprotein component of NADPH oxidase (Fig. 5D). Treatment of caveolin −/− MPMVEC with thrombin led to a similar increase of DCF fluorescence as in wild type cells indicating that they are capable of generating ROS via NADPH oxidase (Fig 5D). These results indicate that caveolin-1 is “upstream” from NADPH oxidase activation during the response to ischemia.

Phosphorylation of MAP kinases with simulated ischemia

As our studies suggest that signaling through caveolin-1 occurs with flow cessation, we evaluated possible activation of MAP kinases under these conditions using specific antibodies. We previously have demonstrated in bovine pulmonary artery endothelial cells that ischemia results in phosphorylation of ERK 1/2 [14]. In the present study, ischemia for 15 min resulted in a 4-fold increase in phosphorylation level of Erk as well as JNK (Fig. 6A, B). There was no change in the phosphorylation level of p38 associated with ischemia (data not shown). The increased phosphorylation of Erk/JNK was markedly diminished in $gp91^{phox}$–/– cells (Fig. 6A, B), indicating that ROS generation with ischemia is required for activation of the MAP kinases in MPMVEC as previously shown for bovine cells [14]. The specific inhibitors, PD98059 for Erk and U0126 for JNK, markedly depressed ischemia-mediated phosphorylation of the target kinases (Fig. 6C, D). Okadaic acid and cyclosporin A treatment resulted in increased Erk and JNK phosphorylation, presumably due to inhibition of phosphatases while orthovanadate had no effect (Fig. 6C, D). This result suggests specificity of phosphatases in these cells towards phosphorylated MAP kinases. Erk/JNK phosphorylation with ischemia was not observed in caveolin-1 −/− cells (Fig. 6 A,B) or in wild type cells pretreated with filipin (Fig. 6 C,D) and levels in the null cells were unchanged by the phosphatase inhibitors (not shown).

Cellular proliferation and cell cycle with simulated ischemia

Proliferation of MPMVEC seeded at a sub-confluent density (1×10^6 per cartridge) was evaluated after culture for 96 h under static conditions or with continuous laminar flow (5 dynes/cm^2). The proliferation index (PI) of cells at day 0 was set to 1.0. As previously shown

[5,6], the fluorescence distribution of wild type MPMVEC cultured in cartridges under static conditions demonstrated multiple peaks indicating several generations of cell division (not shown). On the other hand, the fluorescence distribution for cells cultured for 96 h under flow showed a single peak (Fig. 7A) indicating a lack of cell division. These results are compatible with flow-mediated inhibition of cell division as observed previously [5,6,22]. The proliferation index of wild type MPMVEC significantly increased with ischemia (Fig. 7A). Prolilferation was markedly attenuated with filipin pretreatment (Fig. 7A). The proliferative response with ischemia also was markedly attenuated in caveolin-1 null cells (Fig. 7A). These results indicate a requirement for ROS in order to initiate cell proliferation following ischemia as shown by our previous studies [5,6]. The MAP kinase inhibitors PD98059 and UO126 significantly attenuated cell proliferation (Fig. 7B). Treatment of wild type cells with the phosphatase inhibitors okadaic acid and cyclosporine A significantly increased proliferation (Fig. 7B) suggesting that protein phosphorylation is important in the signaling cascade. Vanadate had no effect (Fig. 7B). This response to phosphatase inhibitors shows the same pattern as seen for MAP kinase phosphorylation (Fig. 6C, D). The PI with ischemia did not increase in the caveolin-1 null cells even in the presence of phosphatase inhibitors (Fig. 7B).

The yield of cells obtained by trypsinization from the cartridges was used as another index of cell proliferation. There was a marked increase in the cell yield in ischemia compared with continuous flow (Fig. 7C). This reponse was inhibited with filipin pretreatment and abrogated by caveolin-1 knock-out (Fig. 7C). These results confirm those obtained with the flow cytometry method.

Cell cycle analysis of wild type flow-adapted MPMVEC during continuous flow showed fewer than 10% of cells in the S+G_2/M phases; with the observed ischemia, the % of cells in S+G_2/M increased to 35% (Fig. 8). These results are compatible with ischemia mediated cell proliferation. Caveolin-1 null cells showed a high percentage in the G_2/M phase in both confluent (Fig. 8) and subconfluent (not shown) populations with no significant change in cell cycle distribution in response to ischemia (Table 2).

To further evaluate the effect of caveolin-1 knock-out, we treated sub-confluent cells for 12 h with nocodazole, an agent known to cause disruption of microtubles and G_2/M arrest. Wild type and $gp91^{phox-/-}$ MPMVEC showed an increase in the percent of cells in the G_2/M phases reflecting G_2M arrest while the percent of caveolin null cells in G_2/M was unchanged (data not shown). These results are compatible with a relative cell cycle arrest for proliferating caveolin-1 null cells.

DISCUSSION

The present study confirms our previous results which showed that abrupt cessation of shear in intact lungs or to flow adapted endothelial cells results in the production of ROS [1–8] Knock-out of $gp91^{phox}$ results in loss of ROS generation with ischemia indicating that NOX2 is the responsible oxidase [4,6,8,19]. This effect appears to be initiated by endothelial cell membrane depolarization and knock-out of the K_{ATP} channel (K_{IR} 6.2 null cells) attenuates membrane depolarization, although other channels may maintain a partial response. The depolarization response also is abolished by K_{ATP} channel agonists such as cromakalim and we have postulated that these agents prevent channel closure with ischemia [3,15,19]. K_{ATP} knock-out or treatment with cromakalim abrogates ROS generation indicating that cell membrane depolarization precedes activation of the NADPH oxidase. Finally, cell proliferation is subsequent to ROS generation and is prevented by manipulations that alter activation of the oxidase.

The use of ROS scavengers indicates that the major signaling oxidant during ischemia is H_2O_2 since the effect is abolished by the presence of catalase but is relatively unaffected by SOD. However, the initiating oxidant is the superoxide anion which is produced by NOX2 and is then dismutated to H_2O_2. NOX2 produces $O_2^{-\cdot}$ on the extracellular side of the cell membrane but the H_2O_2 product can rapidly transverse the cell membrane for intracellular signaling. These pathways for the signaling response to ischemia are shown schematically in Fig. 9.

The major goal of the present study was to determine the role of caveolae in the endothelial response to abrupt reduction of shear stress. Caveolae previously have been described as an endothelial cell shear sensor in models of increased shear [9–11,23,24]. The impaired response to increased shear was corroborated in the present study by the failure of K_{IR} induction during the flow adaptation period in caveolin-1 null cells. The role of caveolae in ischemia (decreased shear) was evaluated in the present study using cells from mice with knock-out of caveolin-1, the major cytoskeletal protein of caveolae, and by treatment of cells with filipin, a cholesterol trapping reagent that disrupts caveolar function. Knock-out of caveolin-1 abrogated the responses to acute cessation of flow; there was essentially no depolarization of the cell membrane (Fig. 4), no ROS generation (Fig. 5), and no cell proliferation (Fig. 7 and Fig 8). Less extensive studies with filipin showed similar effects. Studies of isolated perfused lungs from caveolin-1 null mice (Fig. 1) corroborated the results with the cell culture system. Wild type and caveolin-1 null cells had similar increase of ROS production in response to thrombin, an agent that does not require caveolae for activation of NADPH oxidase. This result indicates that the activation machinery for the oxidase is present in caveolin-1 null cells. Since the oxidase is not activated by loss of shear in these cells, they appear to have specifically lost the ability to respond to mechanotransduction. As this and our previous studies show, activation of NADPH oxidase with ischemia requires preceding endothelial cell membrane depolarization [3,5,6,8,15]. The failure of caveolin-1 null cells to depolarize with ischemia may reflect in part their significantly lower level of K_{IR} 6.2 compared to wild type in the flow adapted cells; thus, it is not possible to determine in the caveolin-1 null cells the relative roles of altered flow sensing by caveolae vs. altered membrane depolarization in the loss of the downstream responses. On the other hand, abrogation of the ischemic response by pretreatment with filipin provides evidence that functional caveolae are indeed necessary. Coupling between caveolae and activation of NADPH oxidase has been demonstrated for other stimuli, including endothelin-1 in HUVEC [25] and angiotensin II in vascular smooth muscle cells [26,27]. Whether these responses also require depolarization of the plasma membrane is not known.

Abrupt reduction of shear resulted in phosphorylation of MAP kinases, specifically Erk and JNK, which required the presence of caveolae as it was abolished by caveolin-1 knock-out. Phosphorylation of Erk/JNK with ischemia was not observed in NOX2 null cells (Fig. 6) and was depressed in the presence of ROS inhibitors/scavengers [14]. Thus, the signaling pathway leading to ERK/JNK activation appears to require activation of NOX2 with ROS production. Recent studies indicate a role for Ras in ROS-mediated ERK 1/2 activation [28,29] and ROS have been shown to regulate the Ras/Raf-1/ERK pathway with cyclic strain in endothelial cells [30]. Lipid rich domains such as those comprising caveolae and lipid rafts have been proposed as redox signaling platforms where NADPH subunits and related proteins cluster in response to various stimuli [31]. We propose that the caveolar-associated mechanotransduction platform that is formed in association with the altered shear stress of abrupt ischemia includes the K_{ATP} channel proteins in addition to NOX2-associated proteins and MAP kinases or other signaling proteins.

The present results confirm our previous studies showing that endothelial cells *in vitro* proliferate in response to simulated ischemia [5,6]. The cell proliferative response required their prior flow adaptation with maximal response in cells adapted to 5 dynes/cm^2 shear stress for 72 h. The mechanism for priming of this response to altered flow may reflect increased

expression of cellular mechanoresponsive elements as both this and a previous study with rat pulmonary microvascular endothelial cells have demonstrated a significant induction of K_{ATP} channels [18] during the flow adaptation period. Further, long term exposure to shear stress in rat pulmonary microvascular endothelial cells led to increased plasma membrane association of caveolin-1 protein [9] although our studies with mouse endothelial cells showed no change in total caveolin-1 expression during flow adaptation. Endothelial cells *in situ* should be flow-adapted normally as they are constantly exposed to shear. Cell proliferation with ischemia requires the signals associated with ROS since it is abolished by inhibition of ROS generation, either through pharmacologic means (cromakalim, DPI) or by molecular manipulation (K_{ATP} or $gp91^{phox}$ knock-out). Generation of ROS with ischemia *in vitro* previously was shown to result in increased DNA synthesis and cell proliferation [5–7]. Indeed, ROS can mediate Ras-induced cell cycle progression and mammalian cell proliferation and have been shown to stimulate angiogenesis [22,32]. An alternative explanation for the present *in vitro* results is that mechanical stress associated with flow results in depletion of cells from the artificial capillaries leading to loss of "contact inhibition", so that cell division resumes when the anti-proliferative effect of shear stress is discontinued. This possibility for the effect of ischemia is unlikely because subconfluent cells grown under static conditions do not show inhibition of proliferation with a K_{ATP} channel agonist or an inhibitor of ROS production [5]. The absence of ischemia-induced proliferation in the presence of cromakalim or DPI and in K_{ATP} channel or NOX2 null cells contrasts sharply with the lack of effect of these agents on the proliferation of subconfluent endothelial cells grown under static conditions [6]. Therefore, the mechanism for initiation of cell division appears to be different for ischemia after flow adaptation versus sub-confluent static cell cultures. We also demonstrated previously that proliferation with ischemia is not a response to endothelial cell death [6].

Exposure of endothelial cells to steady laminar flow has been shown previously and in the present results to decrease cellular proliferation [22,33]. The increase of cells in the G_0/G_1 phase during exposure to shear stress is accompanied by a reciprocal decrease in the number of cells in the S and G_2/M phases, indicating that steady laminar shear blocks a cell cycle event prior to entry into the S phase. Flow cessation (in flow adapted cells) results in the inverse effect, namely entry of cells into the S phase and cellular proliferation. K_{IR} 6.2 and $gp91^{phox}$ null cells showed a failure of entry into the cell cycle with G_1/G_0 arrest. Since caveolin-1 is a negative regulator of the cell cycle [34], its knockout might be expected to result in a proliferative response, but these cells demonstrated G_2/M arrest and abrogation of proliferation with ischemia. Thus, shear stress as sensed by caveolae may play a key regulatory role in maintenance of the endothelial cell population.

In summary, we have shown using an *in vitro* model of oxygenated "ischemia" that flow adapted endothelial cells sense the cessation of flow through a mechanism involving caveolae resulting in a signaling cascade of cell membrane depolarization, NOX2 activation with increased ROS production, activation of MAP kinases (Erk 1/2, JNK) and cellular proliferation. We postulate that this cell proliferative response to altered shear stress represents an attempt at neovascularization in order to restore blood flow to the ischemic tissue.

ABBREVIATIONS

ROS, reactive oxygen species; MPMVEC, mouse pulmonary microvascular endothelial cells; DPI, diphenyleneiodonium chloride; FITC, fluorescein isothiocyanate; DCF, dichlorofluorescein.

ACKNOWLEDGEMENTS

This work was supported by NIH grant HL60290. We thank Drs. Sheldon Feinstein and Dr. J.W. Jaccoberger for helpful suggestions, Dr. Susan Margulies for use of the multiphoton microscope, and Susan Turbitt for typing the manuscript. Results of this study were presented in preliminary form at the Experimental Biology meeting in San Francisco, CA, April 2006 and at the 24th European Congress of Microcirculation in Amsterdam, the Netherlands, September, 2006.

REFERENCES

1. Al-Mehdi AB, Shuman H, Fisher AB. Am J Physiol 1997;272:L294–L300. [PubMed: 9124381]
2. Manevich Y, Al-Mehdi A, Muzykantov V, Fisher AB. Am J Physiol Heart Circ Physiol 2001;280:H2126–H2135. [PubMed: 11299214]
3. Song C, Al-Mehdi AB, Fisher AB. Am J Physiol Lung Cell Mol Physiol 2001;281:L993–L1000. [PubMed: 11557603]Corrigenda, 282: preceding L167, 2002
4. Zhang Q, Matsuzaki I, Chatterjee S, Fisher AB. Am J Physiol Lung Cell Mol Physiol 2005;289:L954–L961. [PubMed: 16280460]
5. Milovanova T, Manevich Y, Haddad A, Chatterjee S, Moore JS, Fisher AB. Antioxid Redox Signal 2004;6:245–258. [PubMed: 15025926]
6. Milovanova T, Chatterjee S, Manevich Y, Kotelnikova I, Debolt K, Madesh M, Moore JS, Fisher AB. Am J Physiol Cell Physiol 2006;290:C66–C76. [PubMed: 16107509]
7. Wei Z, Costa K, Al-Mehdi AB, Dodia C, Muzykantov V, Fisher AB. Circ Res 1999;85:682–689. [PubMed: 10521241]
8. Al-Mehdi AB, Zhao G, Dodia C, Tozawa K, Costa K, Muzykantov V, Ross C, Blecha F, Dinauer M, Fisher AB. Circ Res 1998;83:730–737. [PubMed: 9758643]
9. Rizzo V, Morton C, DePaola N, Schnitzer JE, Davies PF. Am J Physiol Heart Circ Physiol 2003;285:H1720–H1729. [PubMed: 12816751]
10. Yu J, Bergaya S, Murata T, Alp IF, Bauer MP, Lin MI, Drab M, Kurzchalia TV, Stan RV, Sessa WC. J Clin Invest 2006;116:1284–1291. [PubMed: 16670769]
11. Radel C, Carlile-Klusacek M, Rizzo V. Biochem Biophys Res Commun 2007;358:626–631. [PubMed: 17498653]
12. Razani B, Engelman JA, Wang XB, Schubert W, Zhang XL, Marks CB, Macaluso F, Russell RG, Li M, Pestell RG, Di Vizio D, Hou H Jr, Kneitz B, Lagaud G, Christ GJ, Edelmann W, Lisanti MP. J Biol Chem 2001;276:38121–38138. [PubMed: 11457855]
13. Dong QG, Bernasconi S, Lostaglio S, De Calmanovici RW, Martin-Padura I, Breviario F, Garlanda C, Ramponi S, Mantovani A, Vecchi A. Arterioscler Thromb Vasc Biol 1997;17:1599–1604. [PubMed: 9301641]
14. Wei Z, Al-Mehdi AB, Fisher AB. Am J Physiol Heart Circ Physiol 2001;281:H2226–H2232. [PubMed: 11668087]
15. Chatterjee S, Levitan I, Wei Z, Fisher AB. Microcirculation 2006;13:633–644. [PubMed: 17085424]
16. Wei Z, Manevich Y, Al-Mehdi AB, Chatterjee S, Fisher AB. Microcirculation 2004;11:517–526. [PubMed: 15371132]
17. Milovanova T, Chatterjee S, Manevich Y, Kotelnikova I, Debolt K, Madesh M, Moore JS, Fisher AB. American Journal of Physiology - Cell Physiology 2006;290:C66–C76. [PubMed: 16107509]
18. Chatterjee S, Al-Mehdi AB, Levitan I, Stevens T, Fisher AB. Am J Physiol Cell Physiol 2003;285:C959–C967. [PubMed: 12826604]
19. Matsuzaki I, Chatterjee S, Debolt K, Manevich Y, Zhang Q, Fisher AB. Am J Physiol Heart Circ Physiol 2005;288:H336–H343. [PubMed: 15331375]
20. Al-Mehdi AB, Zhao G, Fisher AB. Am J Respir Cell Mol Biol 1998;18:653–661. [PubMed: 9569235]
21. Djordjevic T, Pogrebniak A, BelAiba RS, Bonello S, Wotzlaw C, Acker H, Hess J, Gorlach A. Free Radic Biol Med 2005;38:616–630. [PubMed: 15683718]
22. Irani K, Xia Y, Zweier JL, Sollott SJ, Der CJ, Fearon ER, Sundaresan M, Finkel T, Goldschmidt-Clermont PJ. Science 1997;275:1649–1652. [PubMed: 9054359]
23. Radel C, Rizzo V. Am J Physiol Heart Circ Physiol 2005;288:H936–H945. [PubMed: 15471980]

24. Sedding DG, Hermsen J, Seay U, Eickelberg O, Kummer W, Schwencke C, Strasser RH, Tillmanns H, Braun-Dullaeus RC. Circ Res 2005;96:635–642. [PubMed: 15731459]
25. Dong F, Zhang X, Wold LE, Ren Q, Zhang Z, Ren J. Br J Pharmacol 2005;145:323–333. [PubMed: 15765100]
26. Ushio-Fukai M, Zuo L, Ikeda S, Tojo T, Patrushev NA, Alexander RW. Circ Res 2005;97:829–836. [PubMed: 16151024]
27. Zuo L, Ushio-Fukai M, Ikeda S, Hilenski L, Patrushev N, Alexander RW. Arterioscler Thromb Vasc Biol 2005;25:1824–1830. [PubMed: 15976327]
28. Aikawa R, Komuro I, Yamazaki T, Zou Y, Kudoh S, Tanaka M, Shiojima I, Hiroi Y, Yazaki Y. J Clin Invest 1997;100:1813–1821. [PubMed: 9312182]
29. Hirotsu S, Abe Y, Okada K, Nagahara N, Hori H, Nishino T, Hakoshima T. Proc Natl Acad Sci U S A 1999;96:12333–12338. [PubMed: 10535922]
30. Yeh LH, Park YJ, Hansalia RJ, Ahmed IS, Deshpande SS, Goldschmidt-Clermont PJ, Irani K, Alevriadou BR. Am J Physiol 1999;276:C838–C847. [PubMed: 10199814]
31. Li PL, Zhang Y, Yi F. Antioxid Redox Signal 2007;9:1457–1470. [PubMed: 17661535]
32. Ikeda S, Ushio-Fukai M, Zuo L, Tojo T, Dikalov S, Patrushev NA, Alexander RW. Circ Res 2005;96:467–475. [PubMed: 15692085]
33. Akimoto S, Mitsumata M, Sasaguri T, Yoshida Y. Circ Res 2000;86:185–190. [PubMed: 10666414]
34. Ushio-Fukai M, Alexander RW. Mol Cell Biochem 2004;264:85–97. [PubMed: 15544038]

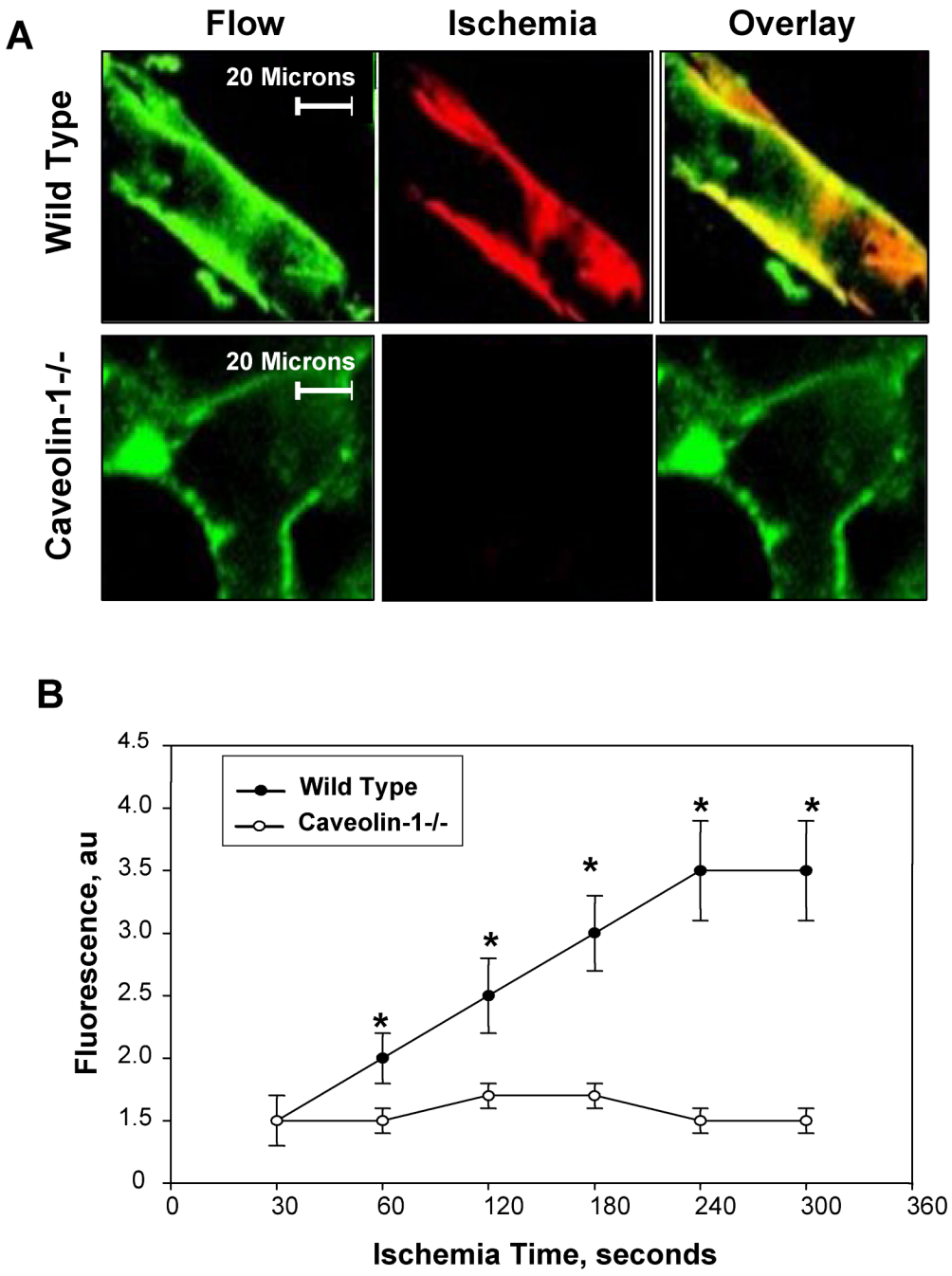

Fig. 1. ROS production with ischemia in the isolated mouse lung

A. Amplex red (ROS sensitive dye visualized in the red channel) and AlexaAcLDL (an endothelial specific marker in the green channel) fluorescence were visualized in endothelial cells in intact wild type and caveolin-1 −/− lungs. Yellow indicates co-localization of the two fluorophores. Images were acquired during perfusion (control) and at 5 min after the stop of flow (ischemia). B. Time course of ROS production during ischemia by wild type and caveolin -1 null mouse lungs. Zero time represents the stop of perfusion. Each point represents the average of 3–4 measurements in a lung field. The results for fluorescence are in arbitrary units (au) and represent the mean ± SE for n=3 separate lungs. *P<0.05 vs. wild type.

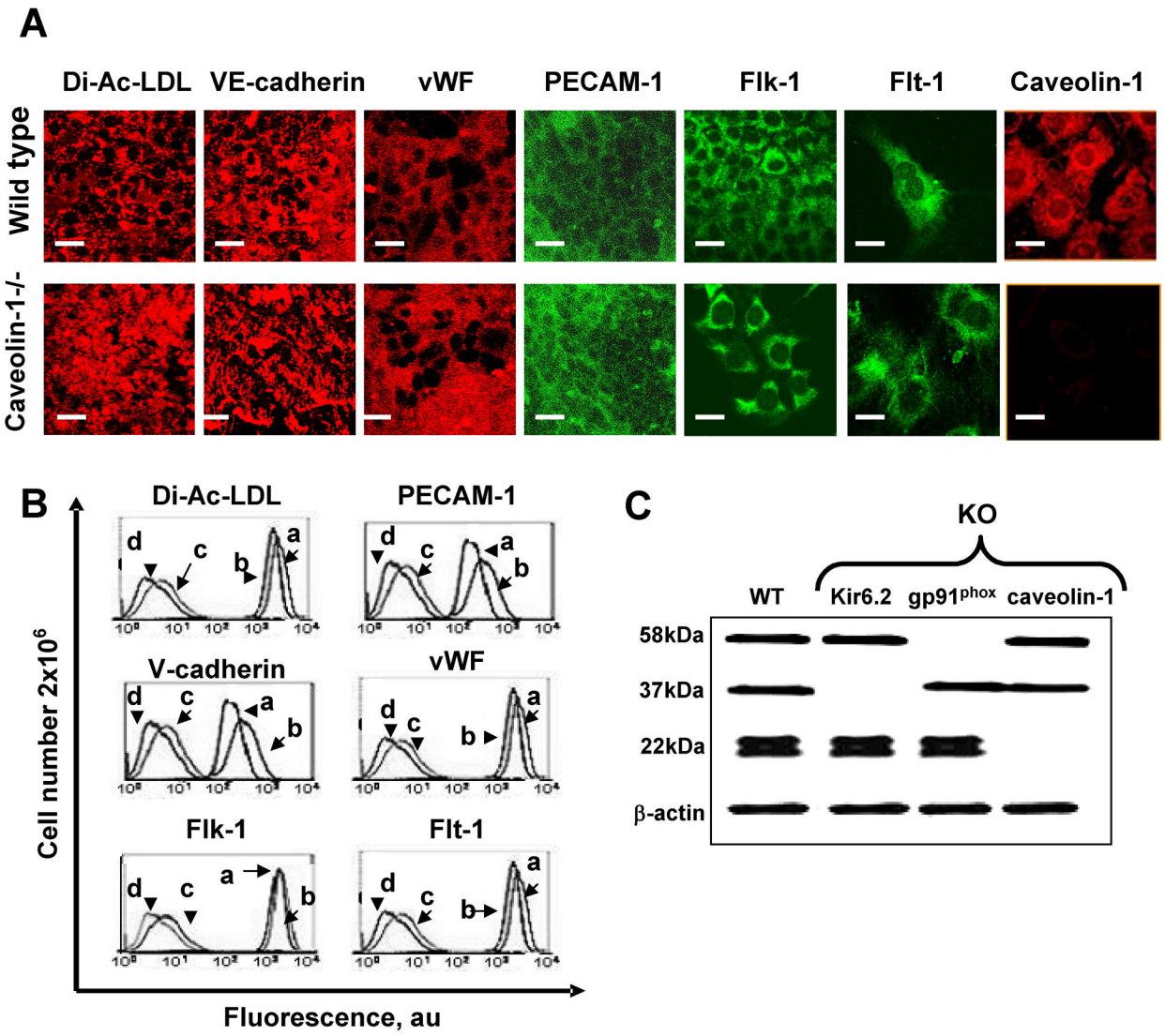

Fig. 2. Phenotype of pulmonary microvascular endothelial cells

A. Images of endothelial cells from wild type and caveolin 1−/− mice with fluorescent DiI-AcLDL, surface immunofluorescence (non-permeabilized cells) with anti-CD31 (PECAM-1), anti-vWF, and anti-caveolin-1 mAbs, and intracellular immunofluorescence cells (permeabilized cells) with anti-VE-cadherin, anti-Flk-1 and anti Flt-1 mAbs. **B**. Flow cytometry histograms for markers shown in A. a, caveolin-1 null cells; b, wild type cells; c, wild type cells without primary antibody (IgG control); d, unstained wild type cells. **C**. Western blot of isolated plasma membrane for gp91^{phox} (58kDa) and cell lysates for Kir6.2 (37kDa) and caveolin-1 (22kDa) protein expression in wild type (WT), K_{IR} 6.2−/−, gp91^{phox}−/−, and caveolin -1−/− cells. β-actin was used as a loading control.

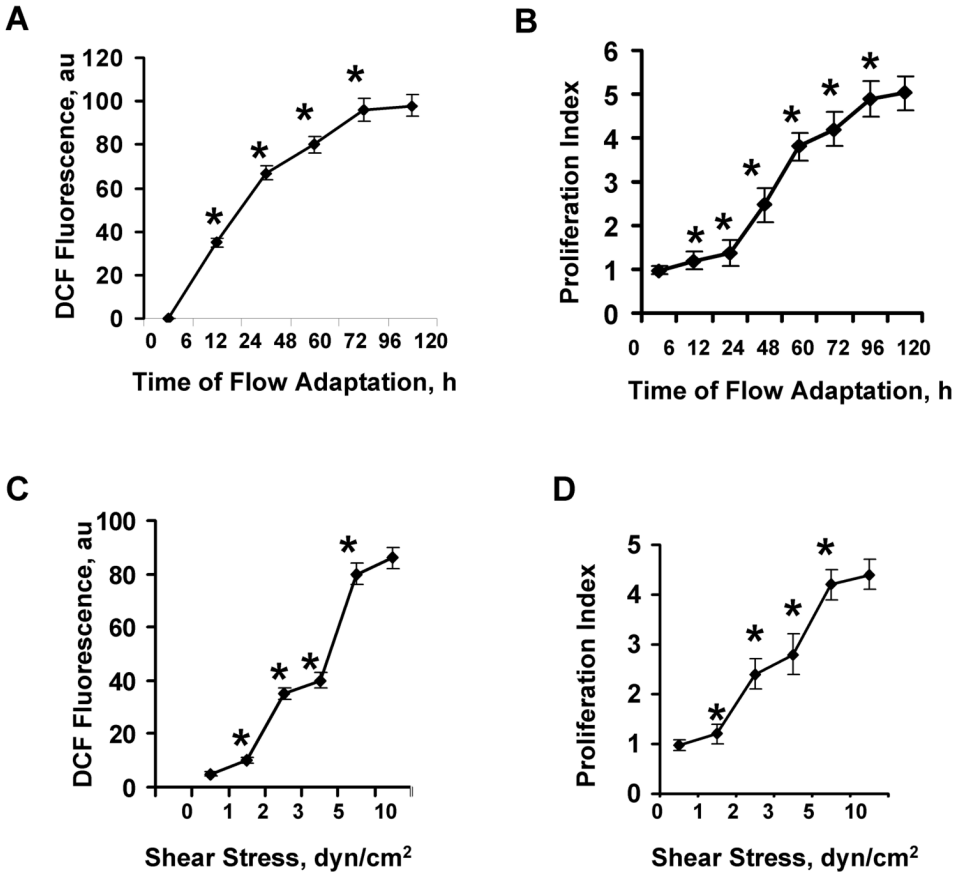

Fig. 3. Response of mouse pulmonary microvascular endothelial cells in vitro to varying duration and magnitude of laminar shear stress

Cells were flow adapted in cartridges and then subjected to 1 h of ischemia for measurement of ROS production by DCF fluorescence or 24 h of ischemia for measurement of cell proliferation using flow cytometry. Results are mean ± SE for n=4. *P<0.05 for the preceding value on the curve. A. ROS production and B. cell proliferation as a function of time of exposure to 5 dyn/cm^2 shear stress. C. ROS production and D. cell proliferation as a function of shear stress following 72 h of exposure to flow.

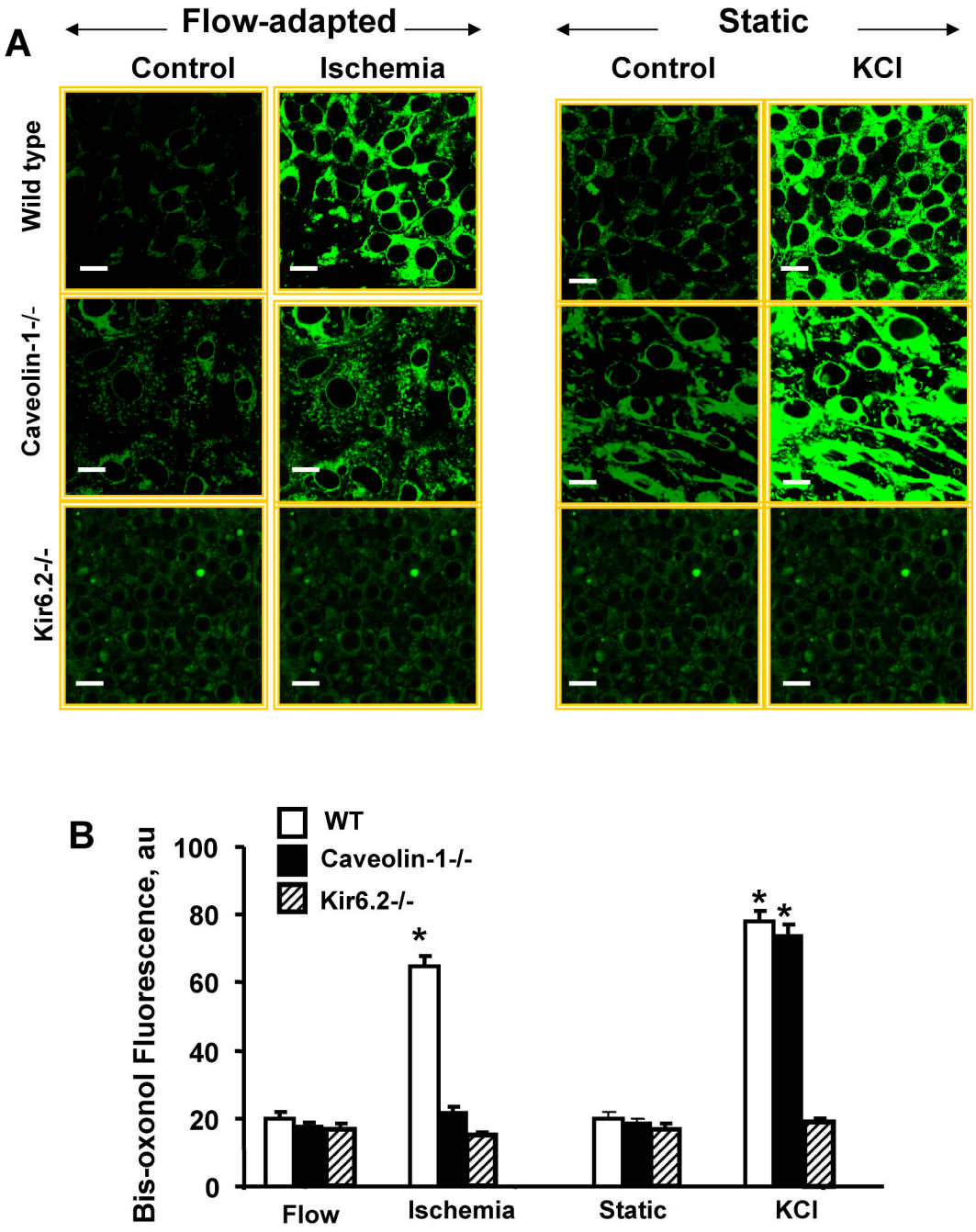

Fig. 4. Membrane depolarization detected by bis-oxonol fluorescence

A. Confocal microscopy of wild type, caveolin-1−/− and K_{IR} 6.2−/− cells loaded with bis-oxonol (200nM). Flow adapted cells were evaluated with continuous flow (control) or 1 hr ischemia. Cells cultured under static conditions were evaluated before (control) and after addition of 24 mM KCl. Cell membrane depolarization is indicated by increased fluorescence. The scale bars indicate 20 μm. **B**. Bis-oxonol fluorescence intensity showing the mean ± SE for n=4 for the experiments described in A. au=arbitrary units.

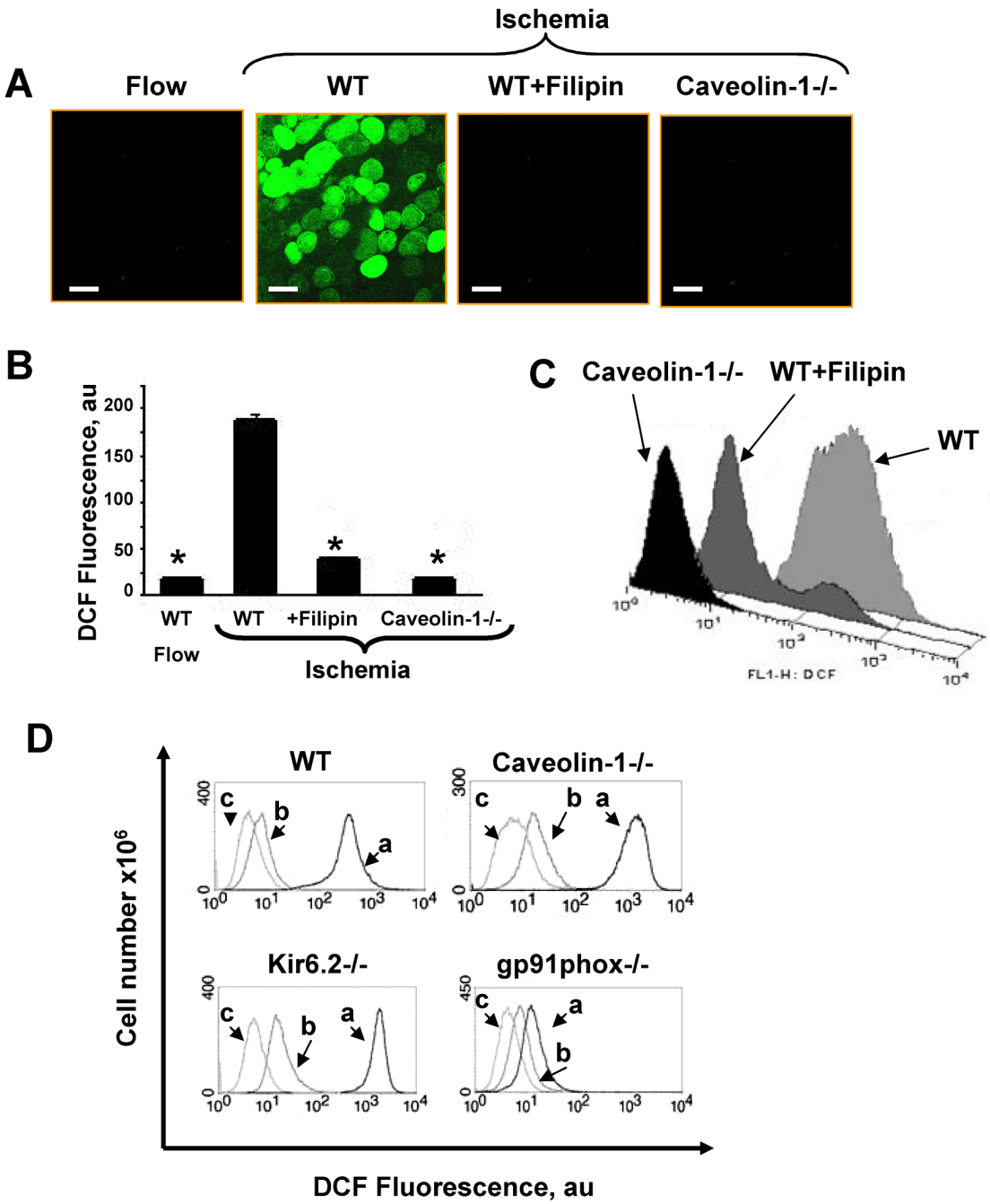

Fig. 5. ROS generation in ischemia as indicated by DCF fluorescence

A. Confocal microscopy of flow adapted wild type (WT) MPMVEC immediately upon cessation of flow (left panel) followed by 1 h of ischemia for WT cells (panel 2), wild type cells pretreated with filipin (1μg/ml) (panel 3), or caveolin-1−/− cells (right panel). The scale bar indicates 10μm. **B**. DCF fluorescence (mean ± SE, n=4) for experiments shown in A. **C**. Flow cytometric analysis of ROS production (DCF-labeled cells) with ischemia for wild type plus or minus filipin and caveolin-1 null. **D**. The effect of thrombin on ROS production by wild type, caveolin-1−/−, Kir6.2−/− and gp91^{phox}−/− MPMVEC cells cultured under static conditions and evaluated by flow cytometry. DCF labeled cells were stimulated with thrombin

(1 unit) for 30 min (a) and compared to unstimulated cells labeled with DCF (b) and non-labeled cells (c).

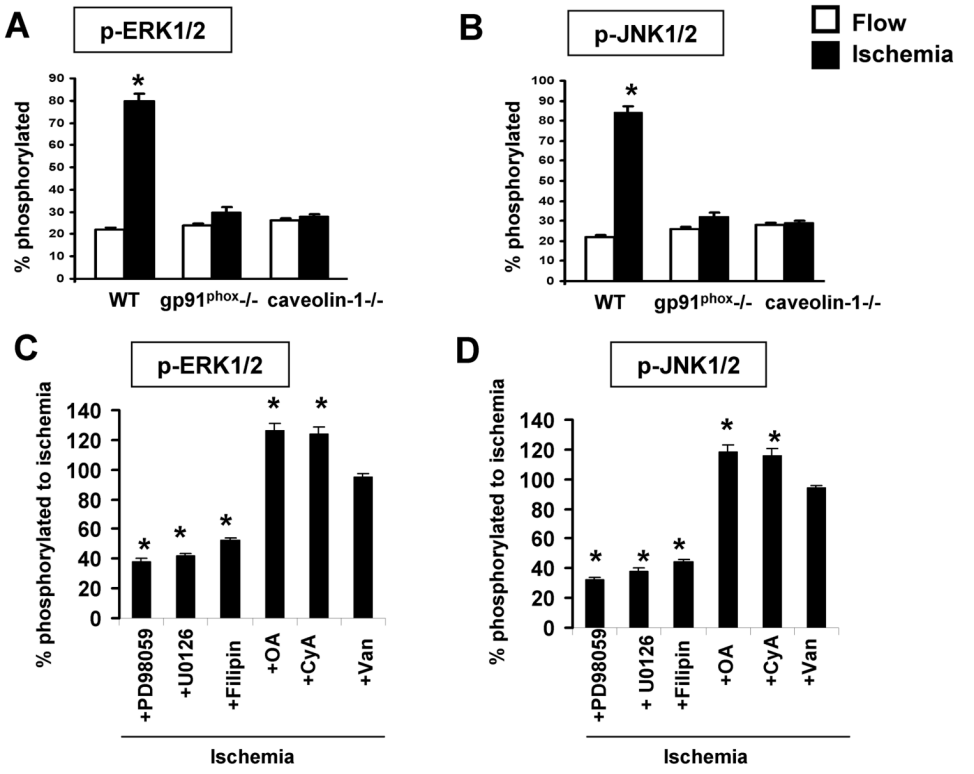

Fig. 6. Phosphorylation of MAP kinases in wild type (WT) and mutant MPMVEC with ischemia (A, B) and the effect of inhibitors (C,D)

Cells were flow-adapted for 72h in the cartridges and fixed during flow or at 15 min after cessation of flow. Cells were collected after trypsinization from the cartridges and phosphorylation of Erk1/2 and JNK1/2 was detected by staining of permeabilized cells. Results are quantified as the fluorescence ratio for phosphorylated vs. total protein. Values are mean ± SE for n=4. The effect of ischemia on phosphorylation of Erk 1/2 (A) and JNK 1/2 (B) is shown for wild type (WT), $gp91^{phox}$ null and caveolin-1 null MPMVEC. *$p < 0.05$ vs. flow. The effect of phosphatase/kinase inhibitors and filipin on phosphorylation of Erk 1/2 (C) and JNK 1/2 (D) during ischemia in flow adapted wild type cells. Results are presented as a % of the corresponding ischemia value shown in A and B. Filipin (1μg/ml); OA, okadaic acid (100nM); CyA, cyclosporine A (100 nM); Van, Na_3VO_4 (100 nM); PD98059 (50 μM); and UO126 (10μM). * $p < 0.05$ vs. ischemia.

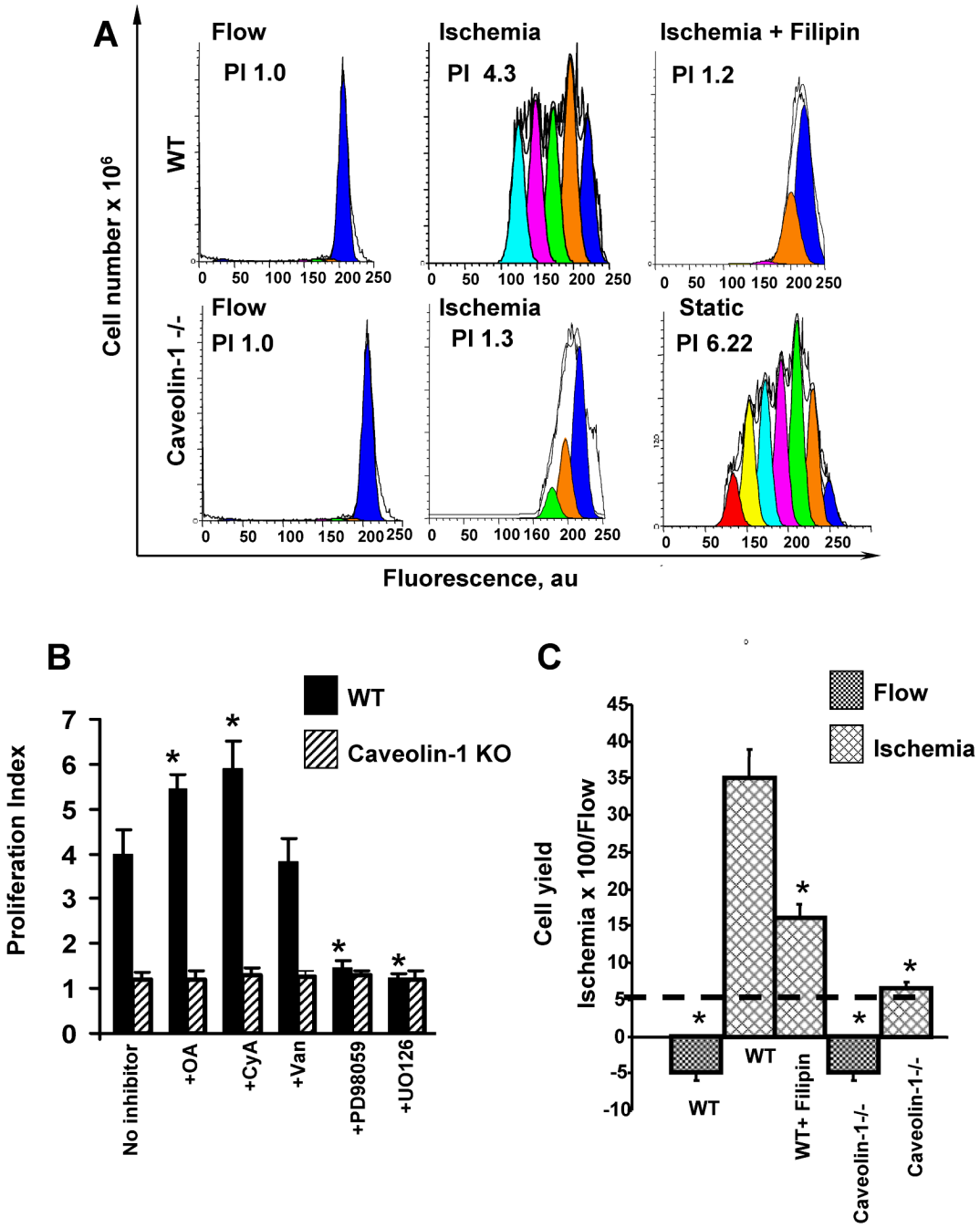

Fig. 7. Effect of ischemia on the proliferation of flow-adapted wild type (WT) and caveolin-1−/− mouse pulmonary microvascular endothelial cells (MPMVEC)

A. Analysis by flow cytometry of PKH26 labeled wild type and caveolin-1 null MPMVEC that were studied during flow and after 24 h of ischemia. Where indicated, filipin (1 μg/ml) was added during the last 30 min of flow-adaptation. Cell proliferation was determined by PKH26 fluorescence intensity of the CD31-positive population using ModFit software. The proliferation index (PI) is indicated in each panel. The PI of caveolin-1 null cells grown under static conditions is shown as a control. B. The effect of phosphatase, protein kinase, and MAP kinase inhibitors on cell proliferation of wild type MPMVEC subjected to 24 h ischemia. The inhibitors were added during the last hour of flow adaptation. The concentrations of inhibitors

were the same as shown in Fig. 6. Control is ischemia in the absence of inhibitors. Values are mean ± SE for n=4. *$p<0.05$ vs the untreated cells. **C**. The % increase in yields (ischemia vs. continuous flow) of cells trypsinized from the cartridges (mean ± SE, n=5) for conditions shown in A.

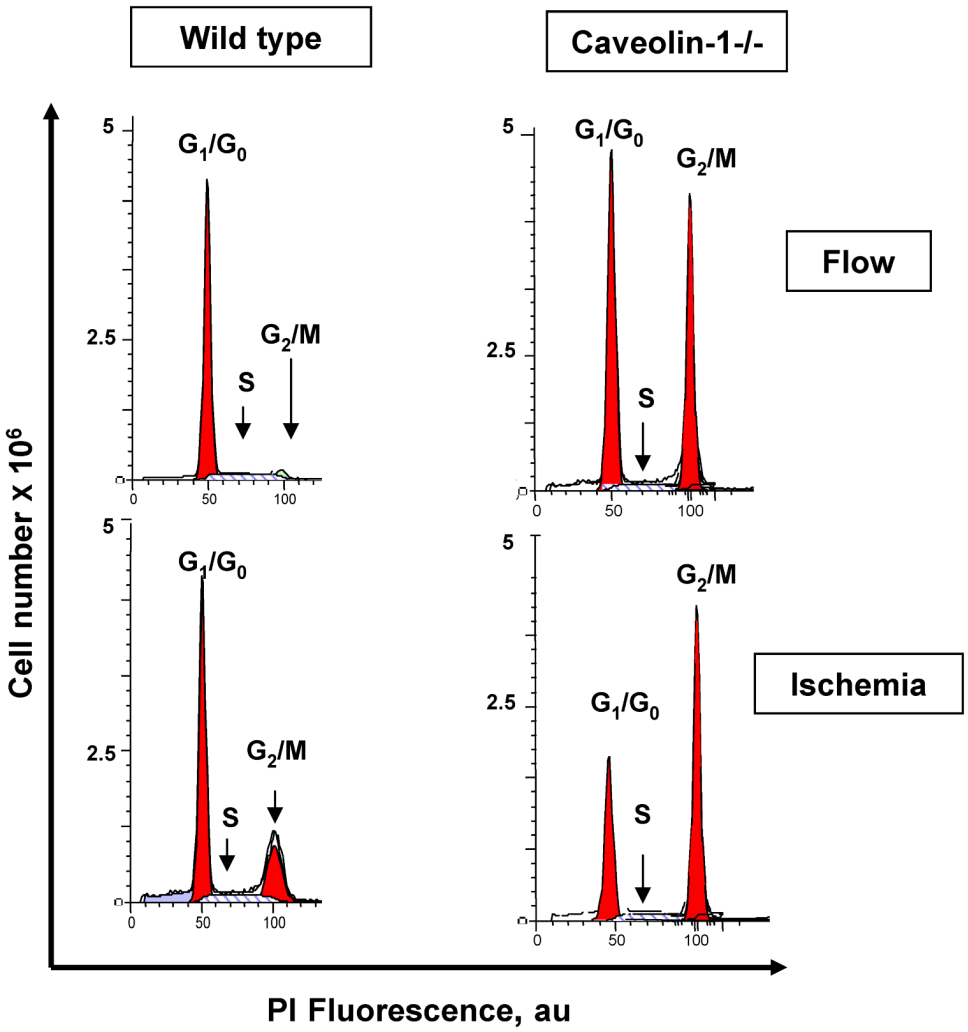

Fig. 8. Analysis of cell cycle for wild type and caveolin-1−/− MPMVEC in response to ischemia

A. Endothelial cells were cultured for 72h under flow followed by 24h of continued flow or 24h ischemia. Cartridges were seeded with 18.0×10^6 cells to promote confluence. The distribution of diploid cells in G_1/G_0, S, and G_2/M phases was evaluated by flow cytometry analysis.

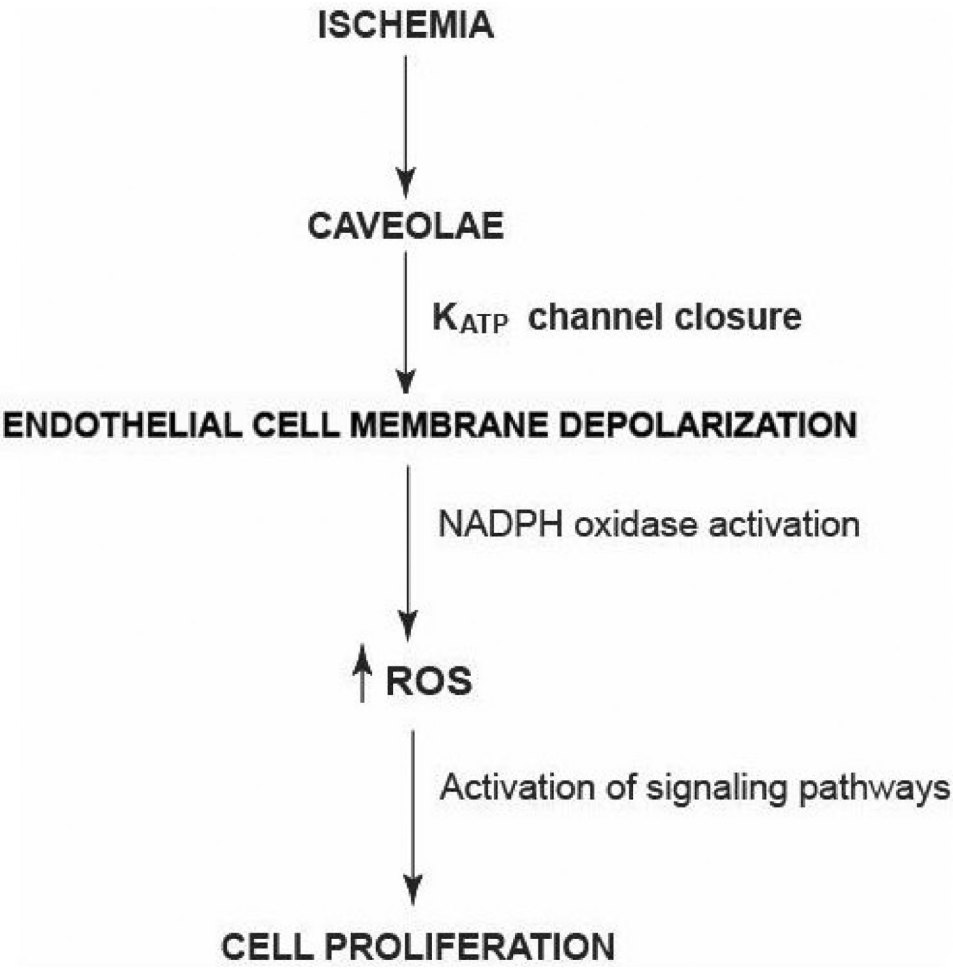

Fig. 9. Scheme for the cell signaling response to ischemia

Altered shear stress is "sensed" by caveolae resulting in K_{ATP} channel closure and cell membrane depolarization. Subsequent activation of NADPH oxidase (NOX2) and downstream signaling pathways results in cell proliferation which may be a compensatory mechanism to restore perfusion.

Table 1

Ratio of the expression levels of protein vs. β-actin by Western blot in static and flow-adapted mouse pulmonary microvascular endothelial cells

Ratio	Static	Flow 72h
Caveolin-1	1.2 ± 0.2	1.2 ± 0.2
$gp91^{phox}$	1.0 ± 0.2	0.9 ± 01.
K_{IR} 6.2	1.0 ± 0.2	3.1 ± 0.3*
ERK 1/2	1.0 ± 0.2	1.0 ± 0.2
JNK 1/2	1.0 ± 0.2	1.0 ± 0.2

MPMVEC were cultured under 5 dyn/cm^2 shear stress for 72 h. Values are mean ± SE for n=4.

Table 2

Distribution of cell cycle phases (%) by flow cytometry in flow adapted mouse pulmonary microvascular endothelial cells during continuous flow and during ischemia

	G0/G_1	**S**	**G_2/M**
Flow			
Wild type	95.11±2.25*	2.98±0.64*	0.96±0.25*
Caveolin-1 Null	53.03±1.43	2.44±0.81	43.92±3.02
Ischemia			
Wild type	60.03±4.87*	16.43±5.16*	24.26±4.05*
Caveolin-1 Null	47.04±3.03	3.56±1.65	47.92±3.17

Cells were cultured under 5 dyn/cm^2 shear stress for 72 h followed by 24 h of ischemia or 24 h of continued flow. Values are mean ± SE for the % of cells in each cell cycle phase (n=4).

* $p<0.05$ vs the corresponding wild type.